Journal of the Physical Society of Japan **86**, 034710 (2017)
https://doi.org/10.7566/JPSJ.86.034710

Neutron Powder Diffraction Study on the Magnetic Structure of $NdPd_5Al_2$

Naoto Metoki[1,2*], Hiroki Yamauchi[1], Hideaki Kitazawa[3], Hiroyuki S. Suzuki[3], Masato Hagihala[4], Matthias D. Frontzek[5], Masaaki Matsuda[5], and Jaime A. Fernandez-Baca[5]

[1]*Materials Sciences Research Center, Japan Atomic Energy Agency, Tokai, Ibaraki 319-1195, Japan*
[2]*Institute of Quantum Beam Science, Graduate School of Science and Engineering, Ibaraki University, Tokai, Ibaraki 319-1106, Japan*
[3]*Research Center for Advanced Measurement and Characterization, National Institute for Materials Science, Tsukuba, Ibaraki 305-0047, Japan*
[4]*Neutron Scattering Laboratory, Institute for Solid State Physics, University of Tokyo, Kashiwa, Chiba 277-8581, Japan*
[5]*Quantum Condensed Matter Division, Oak Ridge National Laboratory, Oak Ridge, TN 37831-6393, U.S.A.*

(Received October 20, 2016; accepted January 10, 2017; published online February 24, 2017)

The magnetic structure of $NdPd_5Al_2$ has been studied by neutron powder diffraction. We observed the magnetic reflections with the modulation vector $q = (1/2, 0, 0)$ below the ordering temperature T_N. We found a collinear magnetic structure with a Nd moment of $2.7(3)\,\mu_B$ at 0.5 K parallel to the c-axis, where the ferromagnetically ordered a-planes stack with a four-Nd-layer period having a $++--$ sequence along the a-direction with the distance between adjacent Nd layers equal to $a/2$ (magnetic space group P_anma). This "stripe"-like modulation is very similar to that in $CePd_5Al_2$ with $q = (0.235, 0.235, 0)$ with the Ce moment parallel to the c-axis. These structures with in-plane modulation are a consequence of the two-dimensional nature of the Fermi surface topology in this family, originating from the unique crystal structure with a very long tetragonal unit cell and a large distance of >7 Å between the rare-earth layers separated by two Pd and one Al layers.

1. Introduction

The heavy-fermion superconductivity in $NpPd_5Al_2$[1)] has attracted strong interest in the field of strongly correlated electron systems. This compound was the first discovered and an only known example of Np-based superconductor. The heavy-fermion nature [electronic specific heat constant $\gamma = 200\,\mathrm{mJ/(K^2{\cdot}mol)}$] has been observed at low temperatures with non-Fermi liquid behavior in the temperature dependence of the resistivity. It becomes superconducting below the relatively high transition temperature of $T_c = 4.9$ K. The xy-type anisotropy in the magnetic susceptibility with the easy plane perpendicular to the tetragonal c-axis suggests the two-dimensional nature of the electronic structure. Remarkable cylindrical Fermi surfaces as well as pancake- or doughnut-like shapes were revealed by a band calculation, where the Fermi level is located at the narrow f-band with a large density of states.[2)] This two-dimensionality is attributed to the unique crystal structure with a very long body-centered tetragonal unit cell ($I4/mmm$) and a very large Np interlayer distance of $c/2 > 7$ Å separated by two Pd layers and one Al layer, while $a \sim 4.1$ Å is also very large. Therefore, it is expected that 5f electrons will retain a localized character. A recent Mössbauer study empirically concluded a Np valence close to the trivalent state Np^{3+} from the isomer shift.[3)] This is consistent with the band calculation, which predicts the number of 4f electrons to be 3.7, roughly corresponding to $Np^{3.3+}$, which slightly deviates from the trivalent state. An NMR study reported d-wave superconductivity mediated by xy-type magnetic fluctuation.[4,5)]

The mechanism of the unusual heavy-fermion nature and the superconductivity as well as the 5f electronic state is of particular interest, but the strict regulation of nuclear materials makes further investigations difficult. For example, the dynamical magnetic correlation remains an open question. In this situation, the isostructural rare-earth family RPd_5Al_2 is helpful for shedding light on the unusual behavior of the Np compound; RPd_5Al_2 (R: Y, Ce, Pr, Nd, Sm, Gd) has been systematically synthesized.[6)] Antiferromagnetic transitions were reported for this series (except for Y compound without 4f electrons and Pr compound with the singlet ground state), where the de Gennes scaling of T_N was more or less confirmed except for $CePd_5Al_2$. The RPd_5Al_2 (R: Tb–Yb) series as well as the new RPt_5Al_2 (R: Y, Gd–Tm, Lu) series has been prepared very recently.[7)] The magnetic structure[8)] and the complicated magnetic phase diagram of $CePd_5Al_2$ have been revealed.[9,10)] An incommensurate sinusoidal modulation with $q = (0.235, 0.235, 0)$ below $T_{N1} = 4.1$ K was reported, while the square modulation was suggested from the observation of the third-order harmonics below $T_{N2} = 2.9$ K. The Ce moment of as large as $2\,\mu_B$ is parallel to the c-axis. Surprisingly, pressure-induced superconductivity in $CePd_5Al_2$ has been reported.[9,10)]

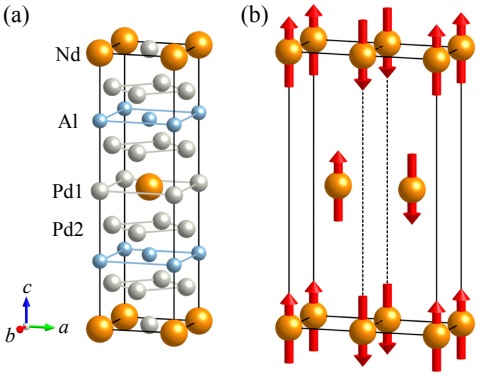

Fig. 1. (Color online) (a) The crystal structure of $NdPd_5Al_2$. (b) The magnetic structure with $q = (1/2, 0, 0)$ and a Nd moment as large as $2.7(3)\,\mu_B$ revealed in this study.

A neutron scattering study of $NdPd_5Al_2$ is highly interesting for clarifying the magnetic correlation in this family. The crystal structure of $NdPd_5Al_2$ is shown in Fig. 1(a). This compound shows antiferromagnetic ordering below the ordering temperature $T_N = 1.2$ K[6)] or 1.3(1) K.[11)]

Figure 1(b) shows the magnetic structure of $NdPd_5Al_2$ revealed in this study. We present the experimental procedures, results, and discussion below.

2. Experimental Procedure

Polycrystalline samples of $NdPd_5Al_2$ were grown by arc melting of stoichiometric amounts of Nd (3N), Pd (3N5), and Al (5N) in a pure Ar atmosphere. A total of 20 g of as-grown samples was mechanically cut in small pieces and sealed in an aluminum can filled with ^{4}He thermal exchange gas. The sample was examined by X-ray powder diffraction and no impurity was detected.

Unpolarized neutron diffraction data were collected on the wide-angle neutron diffractometer WAND (HB-2C) installed at the High Flux Isotope Reactor (HFIR) in the Oak Ridge National Laboratory (ORNL), U.S.A. An incident neutron beam with a wavelength of 1.4827 Å was obtained from a Ge(1 1 3) monochromator. The sample was cooled down to 0.3 K with a ^{3}He cryostat. The diffraction pattern in the paramagnetic state (3.0 K) was analyzed by the Rietveld refinement method with the software Fullprof.[12] The magnetic scattering in the ordered state was also calculated using the same software. The crystal and magnetic structures were drawn with the software VESTA.[13]

3. Results

Figure 2 shows the temperature dependence of the diffraction data of $NdPd_5Al_2$ in the paramagnetic phase at 3.0 K down to 0.3 K in the antiferromagnetically ordered phase. We clearly observed antiferromagnetic reflections below $T = 1.22$ K. The antiferromagnetic reflections disappear above $T = 1.37$ K. The ordering temperature T_N is to be expected between these temperatures, which is consistent with previous studies.[6,11] On the other hand, no remarkable shift or separation of nuclear peaks was detected. This indicates the absence of a significant change in the crystal structure within the sensitivity and resolution of the WAND instrument. We confirmed that the nuclear scattering profile of the paramagnetic phase can be explained with the same

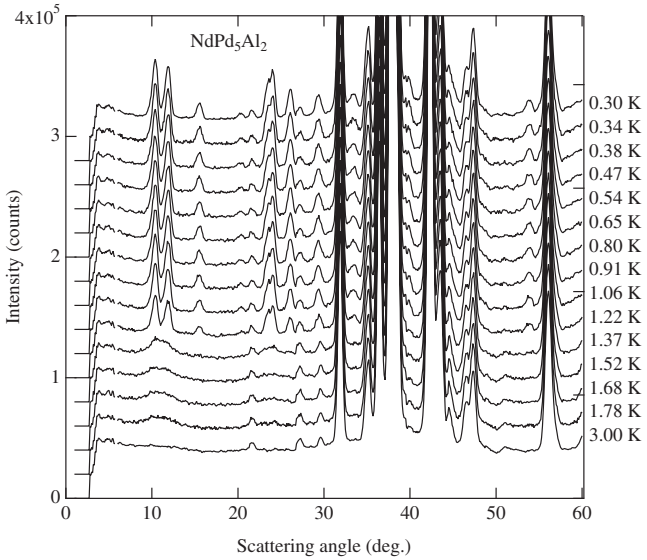

Fig. 2. The temperature dependence of the neutron powder diffraction data of $NdPd_5Al_2$.

crystal structure as that in RPd_5Al_2 (space group $I4/mmm$), where the crystal parameters at 3.0 K were determined as $a = 4.120(1)$ Å and $c = 14.823(2)$ Å with atomic positions Nd($2a$) $(0, 0, 0)$, Pd1($2b$) $(0, 0, 1/2)$, Pd2($8g$) $(0, 1/2, 0.146(1))$, Al($4e$) $(0, 0, 0.257(2))$. Reliability factors were $R_{wp} = 12.0$, $R_e = 4.93$, $R_B = 7.34$, and $\chi^2 = (R_{wp}/R_e)^2 = 5.93$, respectively. All the isotropic atomic displacement parameters B_{iso} were fixed at 0.1 Å^2 during this refinement. The above values are consistent with a recent result of X-ray powder diffraction measured at room temperature.[11]

We observed clear antiferromagnetic reflections, where the peak positions were well explained by the modulation vector of $q = (1/2, 0, 0)$ as shown in Fig. 3. The magnetic contribution was obtained by subtracting the paramagnetic nuclear contribution ($T = 3.0$ K) from the data at $T = 0.5$ K. The peak positions of the observed magnetic reflections are in perfect agreement with those for $q = (1/2, 0, 0)$ as denoted

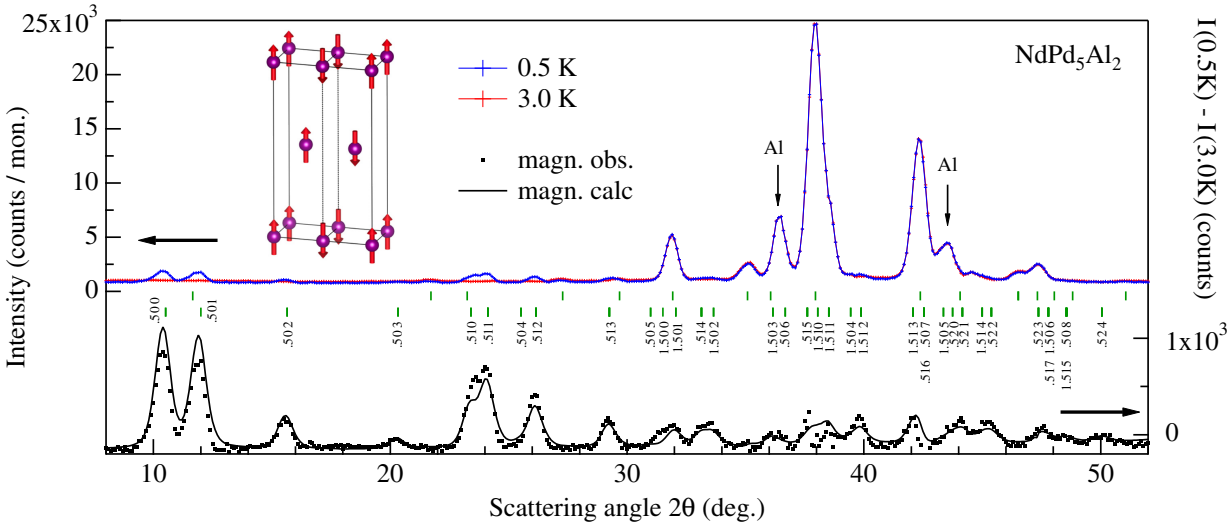

Fig. 3. (Color online) The powder diffraction data of $NdPd_5Al_2$ measured at 3.0 and 0.5 K. The dots and solid line indicate the magnetic contribution obtained by the difference $I(0.5\,\mathrm{K}) - I(3.0\,\mathrm{K})$ and the calculated magnetic diffraction pattern, respectively. The short bars indicate the peak position of the nuclear (upper) and antiferromagnetic (lower) reflections. The inset shows the experimentally determined magnetic structure of $NdPd_5Al_2$.

by short bars. We can clearly recognize that the magnetic intensity decreases significantly with increasing Miller index l. For example, the $(1/2, 0, l)$ reflections with $l = 0$–3 show a significant decrease with increasing l, despite the multiplicity. No peak is recognizable for $l \geq 4$ beyond the statistical error of the background. This result can be understood from the so-called angle factor in the magnetic structure factor calculation. The magnetic component in the plane perpendicular to the scattering vector Q of a neutron contributes to the magnetic scattering. Therefore, the steep decrease in the magnetic scattering with Q approaching the c-direction involves the fact that the Nd magnetic moments are parallel to the c-axis. This is consistent with the Ising anisotropy of the magnetic susceptibility in $NdPd_5Al_2$ with the easy axis parallel to the c-axis.[11] The solid line in Fig. 3 shows the calculated intensities of magnetic reflections, assuming a simple collinear magnetic structure of the Nd moment parallel to the c-axis, consisting of up (+) up (+) down (−) down (−), namely, a ++−− sequence along the a-axis (magnetic space group P_anma), which is schematically shown in the inset of Fig. 3. The magnetic structure factor $(d\sigma/d\Omega)$ is given as

$$\left(\frac{d\sigma}{d\Omega}\right) = 8A^2|M|^2 \sin^2\phi. \quad (1)$$

Here $A = 2.7 \times 10^{-15}$ m is the electronic magnetic-scattering length, and ϕ is the angle between the scattering vector Q and the Nd moment $M = g_J f(Q) J$. $f(Q)$ is the magnetic form factor. A Nd ordered moment of about $2.7(3)\,\mu_B$ at 0.5 K was estimated from the structure factor calculation, typically with $R_{mag} < 11\%$. This large value for Nd compounds is consistent with $g_J J = 3.2\,\mu_B$ for a Nd^{3+} free ion. The somewhat smaller value of the experimentally observed magnetic moment may be understood via a crystalline electric field (CEF) effect.

Strictly speaking, the magnetic structure with the $+0-0$ stacking sequence along the a-axis, namely, Nd atoms on the corner site having magnetic moment but no moment at body-centered positions (magnetic space group, P_amma), provides the same diffraction profile as that calculated using Eq. (1). The scattering cross section in this case also depends only on the angle factor, given as $4A^2|M|^2 \sin^2\phi$. This corresponds to half of Eq. (1), which is due to the absence of the Nd moment at the body-centered site. Then, the Nd moment assuming this structure is obtained as $3.8\,\mu_B$ by multiplying our value of $2.7\,\mu_B$ estimated using Eq. (1) by $\sqrt{2}$. An ordered moment even larger than the effective moment of $3.58\,\mu_B$ for a Nd^{3+} free ion is unrealistic. Furthermore, the observed magnetic entropy $R \ln 2$ released by the antiferromagnetic transition[11] should be half of the observed value when half of the Nd atoms remain paramagnetic below the transition temperature. Assuming a pseudoquartet state to avoid the inconsistency of magnetic entropy again results in disagreement with the moment size.

Since the tetragonal symmetry was broken by the antiferromagnetic ordering, the a- and b-axes are not equivalent in the magnetically ordered phase. However, the difference in the in-plane lattice constant can be undetectably small within rather low angle resolution of the WAND instrument. The collinear structures with $q = (1/2, 0, 0)$, namely, the ++−− or $+0-0$ sequence and the magnetic moments either parallel to the a- or b-axis, are allowed from the group theoretical point of view. Obviously these four structures are ruled out from the present neutron diffraction data. No multi-q structure is allowed for this case of Ising type (M // c) and in-plane modulation $q = (1/2, 0, 0)$, which could maintain the in-plane tetragonal symmetry.

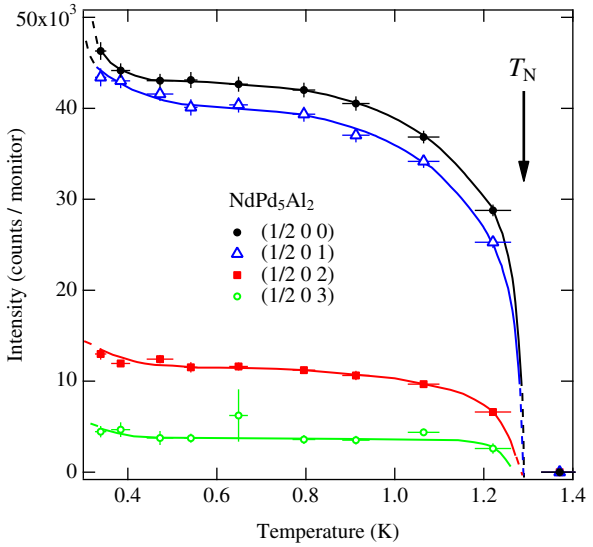

Fig. 4. (Color online) The temperature dependence of the peak intensities of the $(1/2, 0, l)$ antiferromagnetic reflections for $l = 0$–3 observed for $NdPd_5Al_2$. The intensities were obtained by Gaussian fitting. The lines are guides for the eyes.

Figure 4 shows the temperature dependence of the $(1/2, 0, l)$ antiferromagnetic peak intensity for $l = 0$–3. We observed remarkable increases in the intensities with decreasing temperature. A small enhancement of the magnetic scattering intensity below 0.5 K can be interpreted as the hyperfine enhancement of ^{143}Nd and/or ^{145}Nd nuclei (both $I = 7/2$) with natural abundances of 12.2 and 8.5%, respectively. The cross section of the hyperfine term is proportional to the incoherent scattering length and the average of the nuclear spin operator. In the case of Nd, both nuclei have strong incoherent scattering, in particular, ^{143}Nd has comparable incoherent scattering to a proton. The procedure for the detailed analysis of this effect has been published in previous studies on, for example, $HoBa_2Cu_3O_7$[14] and $NdFeO_3$.[15] In fact, the hyperfine enhancement has been observed for many Nd compounds.[16] For an unpolarized neutron, the contribution from the hyperfine enhancement provides additional terms to the cross section for the magnetic structure factor in Eq. (1). As mentioned above, it is proportional to the average of the nuclear spin operator. While 0.5 K is too high to allow a fully polarized state, the temperature is low enough to give the average a non-zero value.

Nowadays the hyperfine structure of rare-earth nuclei can be measured by a high-resolution neutron backscattering spectrometer.[16,17] It has been reported that the hyperfine splitting of Nd nuclei can be scaled by the size of the Nd magnetic moment, which provides the internal field at a nuclear site.[16] From the present result of $2.7\,\mu_B$, the splitting between two levels with $\Delta I \pm 1$ is expected to be $\sim$3.5 μeV. The total splitting between $I = \pm 7/2$ can be obtained as $\sim 3.5 \times 7 \simeq 25$ μeV, which roughly corresponds to $\sim$0.2 K,

comparable to the lowest temperature in this study. Therefore, the finite polarization of the nuclear magnetic moment can be realized even in the temperature range attainable by a ^{3}He cryostat, which is rather high for the observation of the nuclear magnetic order. One possible reason for this is that the hyperfine field at the Nd site is very strong in $NdPd_5Al_2$, as suggested by the large value of the Nd moments. It would be interesting to measure the incoherent inelastic contribution in this compound to evaluate the hyperfine field at the nucleus.

As shown in Fig. 4, the nuclear contribution was clear but negligibly small down to 0.3 K. Furthermore, analysis with additional parameters to take the nuclear magnetic contribution into account may not be reliable using the present data with a relatively strong background. Therefore, we estimated the moment size from the data measured at 0.5 K and ignored the nuclear contribution.

4. Discussion

The obtained magnetic structure shown in the inset of Fig. 3 is highly interesting in comparison with that for $CePd_5Al_2$.[8] The projections of the magnetic structures on the c-plane are shown in Fig. 5. The magnetic structure in $NdPd_5Al_2$ consists of $++--$ modulation including four Nd layers in a period as shown in Fig. 5(a). If we assume the incommensurate propagation $q = (0.235, 0.235, 0)$ in $CePd_5Al_2$ to be approximately commensurate with $q = (1/4, 1/4, 0)$, then the magnetic structure is also described by the $++--$ sequence with a four-Ce-layer period but along the [110] direction, as in Fig. 5(b). These "stripe"-like structures break the tetragonal symmetry and cannot be understood in terms of superexchange interactions and the paramagnetic crystal symmetry. Instead, they should be interpreted in terms of the RKKY interaction. It is highly important that both compounds show only in-plane modulation $q_{\parallel}$; the amplitudes $|q_{\parallel}| = 0.33|a^*|$ for $CePd_5Al_2$ and $0.5|a^*|$ for $NdPd_5Al_2$ are small and comparable. Cylindrical electron and hole Fermi surfaces have been reported on the basis of the band calculation of 4f-itinerant $CePd_5Al_2$ and the non-4f reference compound $LaPd_5Al_2$, respectively.[10] The experimentally observed Fermi surfaces in $CePd_5Al_2$ and $PrPd_5Al_2$ have been reported to be similar to those for $LaPd_5Al_2$,[10] which reflect the Fermi surface topology of RPd_5Al_2 with localized 4f electrons. Namely, 4f electrons in $CePd_5Al_2$ and $PrPd_5Al_2$ are well localized. The dominant RKKY interaction mediated by the conduction electrons with cylindrical Fermi surfaces can be expected to be described by the modulation only with the in-plane component $q_{\parallel}$ as observed in $CePd_5Al_2$ and $NdPd_5Al_2$ in a previous and the present study, respectively. The exact size and in-plane direction of the propagation vector may depend on the size of the Fermi surface as well as the interaction Hamiltonian including 4f and conduction electron orbitals, and thus the detail of the electronic structure.

According to the mean-field calculations for $CePd_5Al_2$ and $PrPd_5Al_2$, the Ising-type magnetic anisotropy can be interpreted as the local properties of 4f electrons, namely, the CEF effect. We consider that this is also the case for $NdPd_5Al_2$, although the CEF level scheme has not yet been proposed. The Ising-type anisotropy is a common feature, which was also revealed in a recent study on high-quality single crystals of $NdPd_5Al_2$.[11] This common feature can be interpreted from the unique crystal structure in Fig. 1(a). The rare-earth elements sandwiched by two Pd and Al ligand layers exhibit a two-dimensional nature with the 4f orbitals elongated within the c-plane. Consequently, the wave functions with a flat orbital and large J_z become dominant. Thus, the Ising anisotropy is expected. Note that the orbital moment is dominant in rare-earth ions. In addition, the relatively large ordered moment of $NdPd_5Al_2$ as well as that of $CePd_5Al_2$ along the quantization axis of the tetragonal c-axis can also be understood in a similar manner.

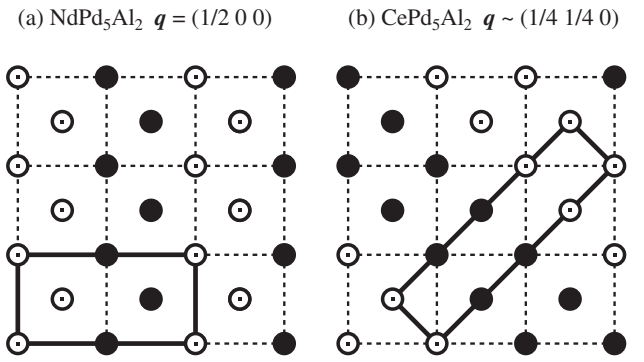

Fig. 5. The projections of the magnetic structures on the tetragonal c-plane for (a) $NdPd_5Al_2$ and (b) $CePd_5Al_2$. The open and closed circles denote spin-up and -down, respectively. The dotted lines indicate the chemical unit cell, while the solid lines denote the magnetic unit cell.

On the other hand, it has been argued that $NpPd_5Al_2$ with xy-type anisotropy is somewhat different from the situation of the rare-earth-based reference compounds, which may be related to the unusual physical properties of $NpPd_5Al_2$;[10] for example, d-wave pairing mediated by this xy-type magnetic fluctuation was pointed out in NMR studies.[4,5] However, we can expect that a rather strongly localized nature remains in $NpPd_5Al_2$ because of the unique crystal structure with very large inter- and intraplane distances between Np atoms. Further study of $NpPd_5Al_2$ as well as the isostructural family is required to shed light on the electronic properties of f electrons.

5. Conclusions

The magnetic structure of $NdPd_5Al_2$ was determined to have the propagation vector $q = (1/2, 0, 0)$ and a Nd moment parallel to the c-axis, similar to that for $CePd_5Al_2$. In both cases, the in-plane modulation can be understood by the two-dimensional nature of the Fermi surface topology with dominant cylindrical Fermi surfaces, which provide important information on the dynamical magnetic correlation in the heavy-fermion superconductor $NpPd_5Al_2$.

Acknowledgment

We thank the US–Japan Cooperative Program on Neutron Scattering using resources at HFIR, operated by ORNL and sponsored by the Scientific User Facilities Division, Office of Basic Energy Sciences, US DOE.

*metoki.naoto@jaea.go.jp

1) D. Aoki, Y. Haga, T. D. Matsuda, N. Tateiwa, S. Ikeda, Y. Homma, H. Sakai, Y. Shiokawa, E. Yamamoto, A. Nakamura, R. Settai, and Y.

Ōnuki, J. Phys. Soc. Jpn. **76**, 063701 (2007).
2) H. Yamagami, D. Aoki, Y. Haga, and Y. Ōnuki, J. Phys. Soc. Jpn. **76**, 083708 (2007).
3) K. Gofryk, J.-C. Griveau, E. Colineau, J. P. Sanchez, J. Rebizant, and R. Caciuffo, Phys. Rev. B **79**, 134525 (2009).
4) H. Chudo, H. Sakai, Y. Tokunaga, S. Kambe, D. Aoki, Y. Homma, Y. Shiokawa, Y. Haga, S. Ikeda, T. D. Matsuda, Y. Ōnuki, and H. Yasuoka, J. Phys. Soc. Jpn. **77**, 083702 (2008).
5) H. Chudo, H. Sakai, Y. Tokunaga, S. Kambe, D. Aoki, Y. Homma, Y. Haga, T. D. Matsuda, Y. Ōnuki, and H. Yasuoka, J. Phys. Soc. Jpn. **79**, 053704 (2010).
6) R. A. Ribeiro, Y. F. Inoue, T. Onimaru, M. A. Avila, K. Shigetoh, and T. Takabatake, Physica B **404**, 2946 (2009).
7) C. Benndorf, F. Stegemann, H. Eckert, and O. Janka, Z. Naturforsch. B **70**, 101 (2015).
8) Y. F. Inoue, T. Onimaru, A. Ishida, T. Takabatake, Y. Oohara, T. J. Sato, D. T. Adroja, A. D. Hillier, and E. A. Goremychkin, J. Phys.: Conf. Ser. **200**, 032023 (2010).
9) F. Honda, M.-A. Measson, Y. Nakano, N. Yoshitani, E. Yamamoto, Y. Haga, T. Takeuchi, H. Yamagami, K. Shimizu, R. Settai, and Y. Ōnuki, J. Phys. Soc. Jpn. **77**, 043701 (2008).
10) Y. Nakano, F. Honda, T. Takeuchi, K. Sugiyama, M. Hagiwara, K. Kindo, E. Yamamoto, Y. Haga, R. Settai, H. Yamagami, and Y. Ōnuki, J. Phys. Soc. Jpn. **79**, 024702 (2010).
11) J. Zubáč, K. Vlášková, J. Prokleška, P. Proschek, and P. Javorský, J. Alloys Compd. **675**, 94 (2016).
12) J. Rodríguez-Carvajal, Physica B **192**, 55 (1993).
13) K. Momma and F. Izumi, J. Appl. Crystallogr. **44**, 1272 (2011).
14) B. Roessli, P. Fisher, U. Staube, M. Zolliker, and A. Furrer, Europhys. Lett. **23**, 511 (1993).
15) J. Bartolomé, E. Palacios, M. D. Kuz'min, and F. Bartolomé, Phys. Rev. B **55**, 11432 (1997).
16) T. Chatterji, G. J. Schneider, L. van Eijck, B. Frick, and D. Bhattacharya, J. Phys.: Condens. Matter **21**, 126003 (2009).
17) T. Chatterji, N. Jalarvo, C. M. N. Kumar, Y. Xiao, and Th. Brückel, J. Phys.: Condens. Matter **25**, 286003 (2013).